Bio-oils Hydrodeoxygenation: Adsorption of Phenolic Molecules on Oxidic Catalyst Supports

Andrey Popov, Elena Kondratieva, Jean Michel Goupil, Laurence Mariey, Philippe Bazin, Jean-Pierre Gilson, Arnaud Travert, and Francoise Maugé*

Laboratoire Catalyse et Spectrochimie, ENSICAEN, Université de Caen, CNRS, 6 Boulevard Maréchal Juin, 14050 Caen Cedex, France

Received: March 4, 2010; Revised Manuscript Received: July 21, 2010

The interaction of phenol, anisole, and guaiacol, representatives of oxygenate functions present in pyrolysis bio-oils, with oxides such as silica, alumina (pure or doped with K or F), and silica−alumina is investigated by infrared spectroscopy. While phenolic type compounds mainly interact via H-bonding with silica, chemisorption is their main mode of adsorption on alumina. Besides, guaiacol interacts very strongly by forming doubly anchored phenates instead of monoanchored ones with phenol and anisole. At temperatures typical of hydrodeoxygenation (HDO) operating conditions (∼673 K), the phenate type species cover 2/3 of the alumina surface. This study clearly indicates that substantial carbon deposition could take place on alumina-supported HDO catalysts. Hence, this suggests that silica-based supports should be considered as potential candidates to design HDO catalyst with better stability.

Introduction

Biofuels are a growing renewable source of energy. To be socially acceptable, their production should use raw materials not competing with the human food chain. These so-called second generation biofuels will mainly rely on liquids derived from pyrolysis of lignocellulosic (waste) biomass. In addition to water, they contain high concentrations of oxygenated molecules.[1,2] Hence, a deoxygenation step is required to produce stable fuels from these oils. Hydrodeoxygenation (HDO) performed on alumina-supported sulfided catalysts is the most promising process for pyrolysis oils upgrading. However, previous studies[1,3−6] highlight severe catalyst deactivation in the HDO process. These works point out that the nature of the support of the sulfide phase affects both activity and selectivity of the HDO catalysts. It was also observed that the support acidity plays a major role in the coking reactions.[7] The interaction of oxygenated molecules with support should lead to the formation of undesired products that could be at the origin of strong deactivation.[8] Substantial quantities of phenolic molecules are present in pyrolytic oil (2−20 wt %[9]) that appear to play a key role in the poisoning of HDO catalysts.[3] It is reported that phenolic double-oxygen compounds such as guaiacol are much more poisoning than single-oxygen compounds such as phenol. However, there is no clear explanation of this effect. Both changes on the support and sulfide phase could be responsible for catalyst deactivation. Hence, to design a HDO catalyst with improved stability, fundamental study of the interaction between the phenolic molecules and the various components of the catalysts has to be done. In this aim, the reaction of oxygenates with various oxides that can be used as potential supports has been studied by infrared (IR) spectroscopy.

Several papers report the studies of the interaction of phenolic compounds with some oxides, although many aspects stay unexplored or unclear.[10−25] IR band assignments mainly referred to previous works done on phenolic compounds in solutions (Table 1).[10−12,15] The adsorption of phenol and anisole on silica was mainly studied at room temperature (RT) and focused on H-bonding between oxygenate and silanol groups.[13,14,16−19] A detailed study by Rochester and co-workers[17,18] of the interaction of phenol or anisole on silica immersed in heptane indicated the formation of H-bonds between the silanols and the aromatic ring or oxygen atom of oxygentates. The interaction of triphenylsilanol and anisole was also reported[20] and validated the previous assignments. No information about strongly adsorbed species on the silica surface was reported as well as their interaction with silica at elevated temperatures. Because HDO reactions take place at high temperatures (>570 K), a detailed study of the adsorption and decomposition of phenolic molecules at relevant temperatures is critical to understand the mechanism of formation of poison species.

TABLE 1: IR Vibrations Characteristic of Pure Phenol, Anisole, and Guaiacol and Their Assignments

assignment	phenol[11,12]	anisole[13]	guaiacol[14]
ν(OH)	3610		3542
$\nu(CH_{ring})$	3074−3021	3105−3037	3059−3008
$\nu(CH_3)$		3004−2834	2936−2846
$\nu(CC_{ring})$	1608	1599	1607
$\nu(CC_{ring})$	1600	1588	1564
$\nu(CC_{ring})$	1502	1497	1508
$\nu(CC_{ring}) + \delta$(OH)[a]	1473[a]		1471[a]
$\delta(CH_3)$		1469−1442	1463−1444[a]
$\nu(CC_{ring}) + \delta$(OH), polymer	1362		
$\nu(CC_{ring}) + \delta$(OH), monomer	1344		1368
X-sensitive $[\nu(CC_{ring}) + \nu(CO)]$	1259	1247	1268, 1229

[a] These data are based on our D-exchange experiments.

Adsorption of phenolic compounds on other oxides than silica is less studied. Taylor at al.[26] and Scire at al.[21] reported that phenol forms chemisorbed species with alumina by a dissociative mechanism. Shabalin and co-workers[22] reported chemi-

* To whom correspondence should be addressed. Tel: +33(0)2 31 45 28 24. Fax: +33(0)2 31 45 28 21. E-mail: francoise.mauge@ensicaen.fr.

10.1021/jp101949j
Published on Web 08/30/2010

TABLE 2: Characteristics of the Oxides

samples	origin and name	S_{BET}[a] ($m^2\ g^{-1}$)	average pore diameter[a] (nm)	V_{porous}[a] ($cm^3\ g^{-1}$)
SiO_2	Degussa, Ultrasil 7000	173	50	0.97
Al_2O_3	Grace-Davison, Catapal C	292	6	0.47
$SiO_2-Al_2O_3$[b]	IFP, Si88Al12	374	7	0.52

[a] Data for samples activated at 673 K. [b] Si/Al = 7.3.

sorbed phenate species on alumina at 573 K for both phenol and anisole but did not discuss their mechanism of formation.

Xu at al.[25] studied phenol adsorption on different oxides displaying various acidic and basic properties, that is, the amorphous $SiO_2-Al_2O_3$, MgO, and ZrO_2 that, respectively, present strong acidic sites, strong basic sites, and weak acidic and basic paired sites. They found that phenate species formed on ZrO_2 are quite stable and related to the presence of both weak acidic and basic sites on the surface. By contrast, the phenol interaction with $SiO_2-Al_2O_3$ and MgO is weaker. According to Tanabe at al.,[23] phenol adsorption on $SiO_2-Al_2O_3$ and MgO leads to phenates formation, and they proposed that their mode of formation depends on the oxide. On acidic $SiO_2-Al_2O_3$, the aromatic ring would be parallel to the catalyst surface interacting with basic π-electrons, while on basic MgO, it would be almost perpendicular.

Literature analysis points out that there is a need for (i) a more systematic study for phenol and anisole adsorption in particular at temperature relevant for HDO reaction, (ii) the extension of these studies to more poisoning molecule as guaiacol, and (iii) the understanding of the effect of oxide acid−base properties on the adsorption modes of these oxygenated molecules. This research on pure oxides will serve as a base for extension to the interaction of oxygenates with supported sulfided catalysts. This second part will be presented in a forthcoming paper.

The present study focuses on the interaction between various phenolic type compounds (phenol, anisole, and guaiacol), with oxides displaying acidic sites of different natures (Lewis or Brønsted) and strength. This is required to establish relationships between the adsorption of oxygenated molecules and the surface properties of metal oxides. Besides silica, pure alumina, alumina modified by the addition of potassium or fluorine, and silica−alumina were tested to determine if modulation of acid−base properties of the support should modify structure, concentration, and stability of the adsorbed species.

Experimental Section

Materials. Commercial oxygen-containing compounds phenol, anisole, and guaiacol were used without additional purification (purity 99.5%, Prolabo for phenol, Johnson Matthey Company for anisole and guaiacol). The origin and the properties of the oxides studied are given in Table 2.

Modified alumina samples (Al_2O_3-K and Al_2O_3-F) were prepared by impregnation of alumina. For potassium addition, a solution of K_2CO_3 (0.066 g/mL for 3% Al_2O_3-K) was added dropwise to the alumina to obtain samples containing 3 wt % K. For fluorine deposition, a NH_4F (concentration 0.035 g/mL) solution was also introduced using the same protocol to obtain a 1 wt % F loading. After impregnation, the samples were dried during one night at 393 K and further calcined at 773 K during 10 h (ramp 3.3 K/min) under air. The textural properties of the modified alumina were close to those of the parent alumina.

IR Spectroscopy Measurement. Each sample was pressed into a self-supported wafer (2 cm^2, between 10−20 mg but precisely weighed), under a pressure of 10^7 Pa. It was then activated by heating from 298 K (RT) up to 723 K (ramp 5 K/min) under vacuum (10^{-4} Pa) and evacuated at this temperature for 3 h. Oxygenated compounds are introduced in the cell at RT using a calibrated volume (1.7 cm^3). Calibrated doses are successively introduced from 0.015 to 0.775 μmol. A final equilibrium pressure of 20 Pa was established in the IR cell. Finally, desorption was carried out from RT up to 723 K with steps of 50 K. At each temperature, the catalyst was evacuated for 10 min prior to recording the IR spectra.

The spectrometer was a Nicolet Magna AEM equipped with a DTGS detector; 64 scans (4 cm^{-1} resolution and one zero filling level) were accumulated for each measurement. Most of the spectra displayed corresponds to difference spectra, that is, spectrum after adsorption (or desorption) minus the spectrum of the corresponding activated sample. All spectra were normalized to a constant mass (10 mg of dry catalysts for a disk of 2 cm^2).

Molar Absorption Coefficient Measurement. The molar absorption coefficients of adsorbed phenol were measured using a combined IR and thermogravimetric analysis (AGIR). A microbalance (from Setaram) was adapted to an IR reactor cell (home designed).[27] The self-supporting wafer (∼10 mg cm^{-2}) placed in the IR reactor cell was continuously weighted (∼1 μg accuracy). The experiment can be split in two steps: (i) activation of the oxides under Ar flow from RT to 673 K (ramp 2 K/min) followed by a cooling down to 473 K and (ii) phenol added to the Ar flow for various times to get increased amounts of adsorbed species.

From simultaneous changes of mass and IR spectra of the sample, the molar absorption coefficient was calculated using the classical Beer−Lambert law:

$$A_i = \varepsilon \frac{n_i}{S}$$

where, for the condition i, A_i is the area of the band (in cm^{-1}); n_i/S is the surface concentration of the species i on the wafer (μmol per cm^2 of wafer), determined from the sample mass measurement; and ε is the molar absorption coefficient (in cm μmol^{-1}).

It should be mentioned that the classical approach (volumetric coupled to IR measurements) used to determine the molar absorption coefficient could not be used due to the very low phenol vapor pressure (53 Pa at RT). This leads to strong inaccuracy in the determination of the amount of phenol introduced in the IR cell. By contrast, the direct measurement of wafer weight changes coupled to IR analysis (AGIR set up) allowed determination of a precise molar absorption coefficient.

Results

Table 1 summarizes the assignments of IR bands of free phenolic oxygenates in solution, which were previously reported in literature.[10−12,15]

Adsorption of Oxygenated Molecules on Silica. ***Anisole Adsorption on Silica.*** The spectra of anisole adsorbed on silica are presented in Figure 1 (spectra a_1 and a_2). In the high

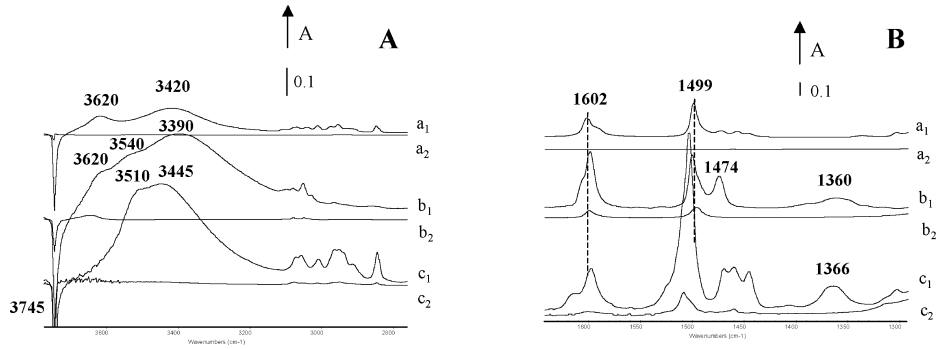

Figure 1. IR spectra of anisole (a), phenol (b), and guaiacol (c) on silica after adsorption at RT at an equilibrium pressure of 20 Pa (a_1, b_1, and c_1), followed by evacuation at 673 K (a_2, b_2, and c_2). (A) High frequency region and (B) low frequency region.

frequency region, anisole adsorption leads to a decrease of free silanol groups (negative band at 3745 cm^{-1}), the appearance of several bands in the range 3100−2800 cm^{-1} related to $\nu(CH_{ring})$ and $\nu(CH_3)$ of anisole (see Table 1), and also of two broad bands at 3620 and 3420 cm^{-1}. In the low frequency region (Figure 1B), characteristic bands of aromatic ring vibration [$\nu(CC_{ring})$] at 1602 and 1499 cm^{-1} and a triplet at 1472, 1456, and 1446 cm^{-1} related to $\delta(CH_3)$ vibrations are observed. Comparison with spectra of anisole in CCl_4 shows very small changes. After evacuation at 373 K, all of the bands corresponding to anisole are eliminated, and simultaneously, the band at 3745 cm^{-1}, characteristic of free silanol groups, is restored.

Phenol Adsorption on Silica. As shown in Figure 1 (spectra b_1 and b_2), the adsorption of phenol on silica leads to a decrease of the silanol band at 3745 cm^{-1} and the appearance of three perturbed OH bands at 3620, 3540, and 3485 cm^{-1}. The frequency of the low wavenumber perturbed OH band shifts toward lower values for increasing phenol coverage (from ∼3485 down to ∼3390 cm^{-1}). No free phenolic OH group at 3610 cm^{-1} (see Table 1) is detected. In the low frequency region (Figure 1B), bands at 1599 (with a shoulder at ∼1606 cm^{-1}) and 1500 cm^{-1} correspond to $\nu(CC_{ring})$ vibrations. The band at 1360 cm^{-1} has a significant contribution of δ(OH) mode (∼20%). The band at 1474 cm^{-1} that is usually assigned to $\nu(CC_{ring})$ vibrations[11,12] also contains a δ(OH) contribution as shown by our IR study of the phenol-OD (not shown). Comparison with the spectrum of pure phenol in CCl_4 provides evidence for a slight shift of all major bands to higher frequencies, appearance of a low frequency shoulder to the band at 1500 cm^{-1}, and some broadening of the band at 1360 cm^{-1}.

After evacuation at 373 K, a large fraction of the perturbed SiO−H bands as well as those at 1474 and 1360 cm^{-1} disappear. However, bands at 1599 and 1496 cm^{-1} can be observed. The band at 1496 cm^{-1} is red-shifted in comparison to the initial band at 1500 cm^{-1} and corresponds to its low frequency shoulder presented during the adsorption stage. The 1599 and 1496 cm^{-1} bands are still present even after evacuation at 673 K (spectrum b_2).

Guaiacol Adsorption on Silica. Spectra of guaiacol adsorbed on silica are shown in Figure 1 (spectra c_1 and c_2). In the high frequency region, the decrease of the free silanol at 3745 cm^{-1} is accompanied by the appearance of two broad bands at 3620 and 3490 cm^{-1}, related to perturbed silanols. At high guaiacol coverage, red shift of the band at 3490 to 3445 cm^{-1} and the appearance of a new band at 3510 cm^{-1} are observed (spectrum c_2). As for phenol, no band of free OH groups of guaiacol at 3555 cm^{-1} is detected, indicating that these groups are perturbed by silanols. In the low frequency region, the spectrum shows bands at 1615, 1598, 1525, and 1504 cm^{-1} similar to those of free guaiacol and related to $\nu(CC_{ring})$ vibrations (see Table 1). The bands around 1470−1444 cm^{-1} are poorly resolved. However, comparison with free guaiacol spectrum reveals some spectral changes with coverage pointing to several adsorption modes. The broad 1366 cm^{-1} band, corresponding to a δ(OH) vibration, is close to that observed for free guaiacol.

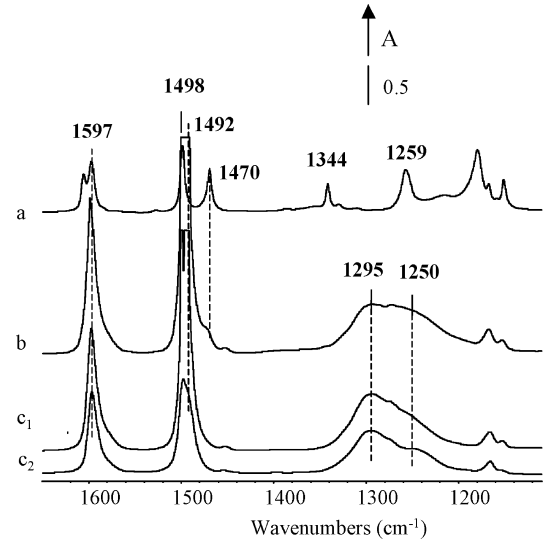

Figure 2. IR spectra of phenol in CCl_4 (a) and on alumina after adsorption at RT at equilibrium pressure of 20 Pa (b), followed by evacuation at 373 (c_1) and 673 K (c_2).

Upon evacuation, a decrease of the 1598 and 1504 cm^{-1} bands reveals the presence of components at 1600 and 1508 cm^{-1}, more difficult to desorb. After evacuation at 673 K (spectrum c_2), bands characteristic of $\nu(CC_{ring})$ vibrations at 1600 and 1508 cm^{-1} and at 1470−1444 cm^{-1} in the region of $\delta(CH_3)$ [and δ(OH)] are still observed, but the δ(OH) contribution at 1366 cm^{-1} disappears.

Adsorption of Oxygenated Molecules on Alumina. ***Phenol Adsorption on Alumina.*** Phenol on alumina (Figure 2) shows main bands at 1597 and 1498/1492 cm^{-1} characteristic of aromatic ring vibrations. For small quantities of adsorbed phenol, the bands at ∼1470 and ∼1340 cm^{-1}, related to δ(OH) vibrations of molecular phenol (spectrum a), are missing. A shoulder at ∼1470 cm^{-1} is only observable for high phenol coverage (spectrum b). After evacuation at 373 K (spectrum c_1), the 1470 cm^{-1} band disappears. A broad multicomponent envelope at 1295/1250 cm^{-1} [ν(CO) vibrations[11,12]] is also observed. The 1250 cm^{-1} component slightly shifts to lower wavenumbers with evacuation temperature and is more resistant to evacuation than the component at 1295 cm^{-1}. These latter bands cannot be observed on silica because of its opacity in this region.

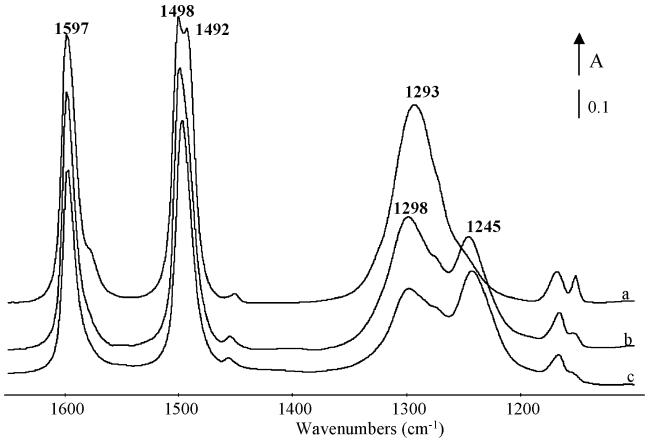

Figure 3. IR spectra of phenol on Al_2O_3−K (a), Al_2O_3 (b), and Al_2O_3−F (c) after adsorption at RT of phenol at equilibrium pressure 20 Pa, followed by evacuation at 673 K.

Adsorption of Phenol on Modified Alumina. Figure 3 presents the spectra of phenol adsorbed at RT and evacuated at 573 K on alumina doped with K (Al_2O_3−K) or F (Al_2O_3−F). The addition of K or F does not lead to strong changes in the ν(CC) vibration zone. However, the ν(CO) zone is markedly modified since the bands at about 1295 and 1245 cm^{-1} have close ratios on pure Al_2O_3 and Al_2O_3−F, while the high wavenumber band dominates on Al_2O_3−K. One can also note a shift of the 1298 cm^{-1} band for Al_2O_3 and Al_2O_3−F to 1293 cm^{-1} for Al_2O_3−K.

Anisole Adsorption on Alumina. Anisole adsorbed on alumina (Figure 4) demonstrates bands specific of aromatic ring at 1593 and 1490 cm^{-1} with shoulders at ∼1600 and ∼1500 cm^{-1} and CH_3 vibrations at about 1458 cm^{-1}. Aromatic ring bands are slightly shifted to low frequency region, and the triplet of CH_3 vibrations is distorted as compared with free anisole (spectrum a).

During stepwise desorption at increasing temperatures (spectra c_1 and c_2), important spectral changes occur at 473−673 K. New $\nu(CC_{ring})$ bands appear at 1596 and 1494 cm^{-1}, while those at 1593 and 1490 cm^{-1} decrease. The effect cannot be explained by a shift of the bands because new components clearly appear during thermodesorption (Figure 4B). Simultaneously, the group of bands at 1458−1440 cm^{-1} of methyl group vanishes. Anisole bands in the region 1300−1150 cm^{-1} also decrease, while two new bands appear at 1295 and 1248 cm^{-1}, at the same position as after phenol adsorption on alumina. In general, the spectra of anisole and phenol on alumina after evacuation at temperatures higher than 473 K are very similar (Figure 4, c_2, and Figure 2, c_2).

Guaiacol Adsorption on Alumina. Upon adsorption of guaiacol (Figure 5), bands at 1615, 1597, and 1504 cm^{-1} [$\nu(CC_{ring})$ vibrations] appear that are similar to those of free guaiacol (spectrum a). At the same time, the 1470−1444 cm^{-1} bands are distorted in comparison with free guaiacol. At low coverage, a band at 1366 cm^{-1} [vibration with δ(OH) contribution] is absent and only appears at higher guaiacol coverage. Bands at 1260 and 1225 cm^{-1} (vibrations with contribution of C−OH and C-OCH_3 stretching modes[15]) still persist along with new bands at 1330 and 1300 cm^{-1}. After a desorption at 373 K (spectrum c_1), the 1470 and 1444 cm^{-1} bands intensity decreases and the 1360 cm^{-1} band disappears. Upon evacuation at 473−673 K (spectrum c_2), further transformations happen as follows: a broadening of the 1597 cm^{-1} band, a low frequency shift of the 1504 to 1497 cm^{-1} bands, a strong decrease of the bands at 1470−1444 cm^{-1}, and changes in C−OH and C−OCH_3 stretching modes at 1350−1200 cm^{-1}.

Adsorption of Oxygenated Molecules on Amorphous Silica−Alumina (ASA). ***Phenol Adsorption on ASA.*** The spectra corresponding to phenol adsorption on ASA (Figure 6) are close to the superimposition of the spectra observed on silica and on alumina, and no additional bands could be noted on ASA.

At low phenol coverage (Figure 6A), the band at 1474 cm^{-1} [δ(OH) vibration] not present on alumina is detected but has a weaker intensity than on silica, although the $\nu(CC_{ring})$ bands have similar intensities on the three samples. At higher coverage (Figure 6B), the spectrum observed on ASA is closer to that of silica than of alumina, likely due to the high silica content (88 wt % SiO_2). The same trend is observed after evacuation at high temperature (Figure 6C).

Adsorption of Anisole on ASA. As previously, no new band of anisole adsorbed on ASA (Figure 7) is detected as compared to silica or alumina. The spectrum at low anisole coverage on ASA (Figure 7A) is similar to that observed for anisole on alumina: two doublets at 1602/1593 and 1499/1490 cm^{-1} are detected. At low coverage, the low wavenumber component presents the highest intensity as on alumina. By contrast, upon increasing anisole coverage (Figure 7B), the high wavenumber component presents the

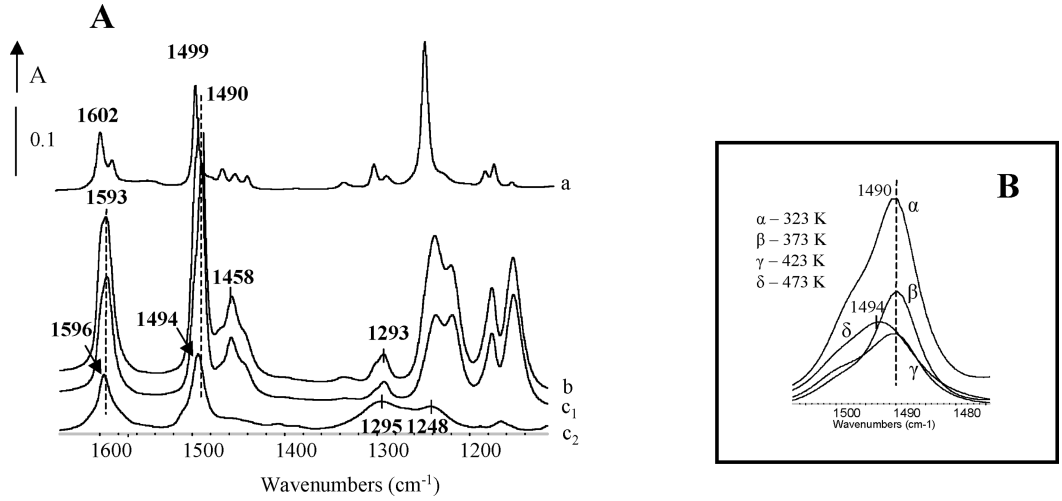

Figure 4. IR spectra of anisole in CCl_4 (a) and on alumina after adsorption at RT at equilibrium pressure of 20 Pa (b), followed by evacuation at 373 K (c_1) and 673 K (c_2). (A) Low frequency region and (B) evacuation at increased temperatures in the region of ∼1500 cm^{-1}.

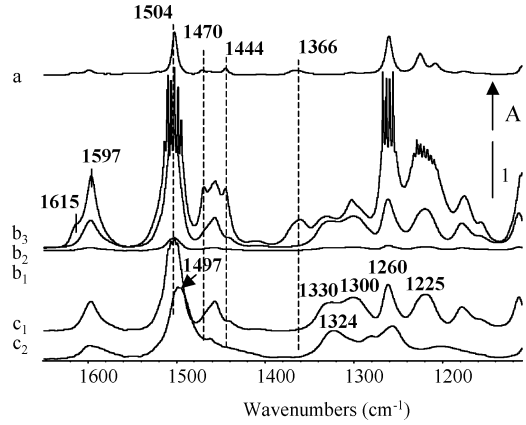

Figure 5. IR spectra of guaiacol in CCl_4 (a) and on alumina after adsorption of 0.005 (b_1) and 0.05 mmol/g (b_2) and of an equilibrium pressure of 20 Pa (b_3), followed by evacuation at 373 (c_1) and 673 K (c_2).

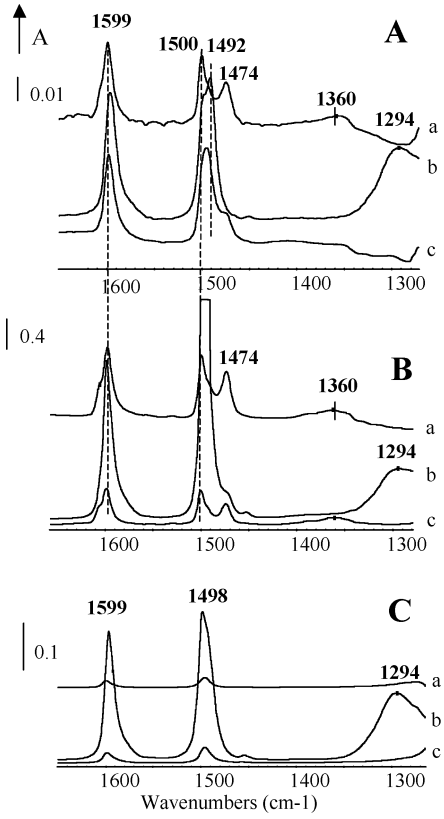

Figure 6. IR spectra of phenol on silica (a), alumina (b), and silica−alumina (c) after adsorption at RT of 0.005 mmol/g of phenol (A), adsorption of phenol at an equilibrium pressure of 20 Pa (B), and after adsorption of phenol at an equilibrium pressure 20 Pa followed by 10 min of evacuation at 673 K (C).

maximum intensity on ASA. After high temperature evacuation (Figure 7C), the low frequency component is again predominant for the two bands, concomitantly with a slight upward shift (1490−1494 and 1593−1596 cm^{-1}).

Determination of Molar Absorption Coefficients. Introduction of phenol flow at 473 K on alumina using the AGIR set up exclusively leads to the formation of phenates in agreement with spectral observations done in the classical set up. Thus, mass increase is only due to phenate species formation. A parallel increase of weight and IR band absorbance with phenate amount allows us to calculate accurately the molar absorption coefficient. For the IR band at 1600 cm^{-1} that is characteristic of aromatic ring vibration of phenate, the value

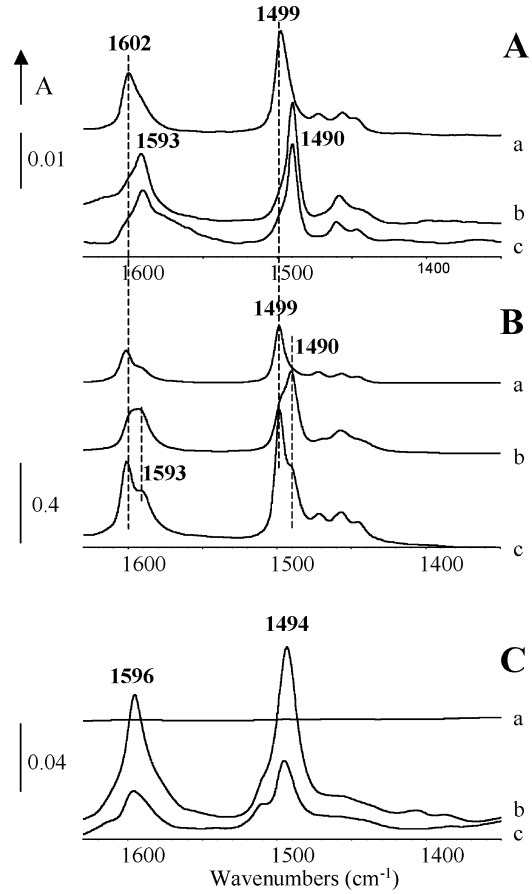

Figure 7. IR spectra of anisole on silica (a), alumina (b), and silica−alumina (c) after adsorption at RT of 0.005 mmol/g of anisole (A), adsorption of anisole at an equilibrium pressure of 20 Pa (B), and after adsorption of anisole at an equilibrium pressure 20 Pa followed by 10 min of evacuation at 673 K (C).

of ε is 5.46 cm μmol^{-1}. It is obtained with a correlation coefficient (r^2) of 0.999.

At high temperature (473 K), anisole also forms phenate species. Hence, the same molar adsorption coefficient may be used for the calculation of the oxygenate concentration after anisole adsorption.

Note that due to the very low vapor pressure of guaiacol, its molar absorption coefficient could not be determined even with AGIR. Moreover, guaiacol interacts with oxides forming methoxy phenate instead of phenate species. The methoxy group should change the molar absorption coefficient of the aromatic ring band, preventing us to use that previously measured for phenate species.

As on alumina, phenol adsorbed at high temperature only forms phenate species on silica and silica−alumina. Thus, the previously measured molar absorption coefficient can be used. This ε value allows us to calculate the concentration of the phenate species formed on the various oxides after treatment by phenol or anisole at 473 K, as presented in Table 4.

Discussion

Oxygenated Molecules on Silica. ***Anisole Adsorbed on Silica.*** The IR spectra of anisole adsorbed on silica indicate H-bonding interactions (Figure 1, spectra a_1 and a_2). As expected, the following features are displayed by very small changes between the spectra of adsorbed anisole and the neat liquid, the desorption starting at 373 K, the perturbation of

SCHEME 1: Different Adsorption Modes of Phenol and Anisole on Silica

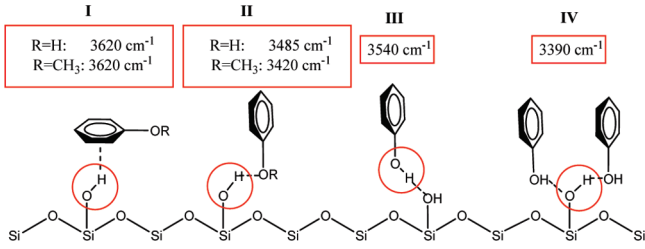

silanol band by anisole adsorption at RT, and its full restoration after anisole desorption. Anisole adsorption gives rise to two SiOH groups perturbed to different extents, that is, 120 and 320 cm^{-1}; the greater the OH group perturbation is, the stronger the H-bonding interaction is. From previous studies of benzene adsorption on silica,[13,14,16] the 3620 cm^{-1} band is assigned to silanol groups perturbed by anisole interaction through its aromatic ring (mode I, Scheme 1), whereas the 3420 cm^{-1} band is attributed to adsorption through the oxygen of anisole (mode II, Scheme 1). Similar conclusions were drawn by Rochester and co-workers for anisole interacting with silica in an heptane solution.[17] However, the adsorption mode whereby two silanol groups interact with the aromatic ring and the oxygen of the same anisole molecule cannot be excluded.

Phenol Adsorbed on Silica. IR spectra of phenol adsorbed on silica provide evidence for H-bonding interaction as well as for stronger adsorption (Figure 1, spectra b_1 and b_2). As for H-bonding, the symptoms are the perturbation of the SiOH band together with the appearance of several related perturbed SiOH bands, especially when adsorption is performed at RT, and the restoration of a large fraction of the silanol band after evacuation at 373 K. The spectra of species adsorbed at RT are very similar to the neat liquid, although differences appear. These are the absence of free phenolic OH group at 3610 cm^{-1} and the shift of the phenol δ(OH) band from 1344 to 1360 cm^{-1} with a broadening and splitting in several components, indicative that phenol's OH groups interact with the surface. A slight upward shift of all of the main bands of aromatic ring vibrations can also be attributed to the interaction between phenol and silica. The two broad bands of perturbed silanol groups at 3620 and 3485 cm^{-1}, close to those observed with anisole (3620 and 3420 cm^{-1}), are assigned to analogous adsorption modes (modes I and II, Scheme 1). The smaller extent of perturbation of SiOH by phenol than by anisole through mode II accounts for the lower electron density on the oxygen atom of the OH group as compared to the methoxy group. The effect of a methyl on the electron density of an aromatic ring seems to be almost negligible. A supplementary band at 3540 cm^{-1}, not observed for anisole, may be assigned to phenolic groups H-bonded to the oxygen atom of SiOH groups (mode III, Scheme 1). They are in agreement with previous studies.[18] However, the frequency shift of mode II from 3485 to 3390 cm^{-1}, not reported previously, leads us to propose an additional adsorption mode (mode IV, Scheme 1), occurring at high phenol coverage. As described in Scheme 1, this species involves the adsorption of two phenols interacting differently, that is, via the oxygen or the proton of its OH group, with the same SiOH group. Hence, increasing phenol coverage should lead to the transformation of species II into species IV—such a transformation explaining the increased perturbation of the SiO−H frequency from ∼3485 to ∼3390 cm^{-1}. A similar type of interaction has been previously reported in the case of H_2S adsorption.[28]

With evacuation at low temperature (not shown), a large fraction of the perturbed SiO−H bands disappears, as well as the bands at 1360 and 1474 cm^{-1}, indicating the elimination of H-bonded phenol. Upon increasing the evacuation temperature, the aromatic ring band intensities slightly decrease, but they always remain, even after evacuation at 673 K (spectrum b_2). The absence of OH band characteristic of phenol as well as the presence of bands characteristic of the aromatic cycle indicate that some phenate species are present on the silica surface. The position of the aromatic ring band at 1496 cm^{-1} slightly differs from the corresponding band of H-bonded phenol at 1500 cm^{-1}, another indication of the formation of phenate species. Moreover, a band at ∼1496 cm^{-1} observed during phenol adsorption stage as a shoulder to the main band at 1500 cm^{-1} further indicates that phenate species are already formed after addition of the first phenol doses. In summary, phenate species form already at RT and remain on the surface even at a temperature as high as 723 K.

A reaction of (inert) silanols with phenol at RT is unlikely. Besides, no water is released during phenol adsorption. Therefore, we propose the formation of phenate on surface defect sites, probably strained siloxane bridges, as proposed in the case of methanol adsorbed on silica.[29] Additional experiments (not shown) show that a pretreatment of silica at 973 K instead of 723 K—increasing the amount of defects on silica surface—increases the amount of phenates on the surface. Thus, phenol on silica interacts through four different types of H-bonded species, as well as through chemisorption, giving rise to phenate species remaining on silica up to 723 K.

Guaiacol Adsorbed on Silica. As phenol, guaiacol interacts with silica through various types of H-bonding and also forms phenate species (Figure 1, spectra c_1 and c_2). The perturbed OH band at 3620 cm^{-1}, close to the one observed for phenol and anisole (at 3620 cm^{-1}), is assigned to silanol groups perturbed by an aromatic ring (Scheme 1, mode I). An intense but poorly resolved band at 3490 cm^{-1} is also observed. By comparison with phenol and anisole, this broad band can be due to the superimposition of bands corresponding to silanols perturbed by OH and by methoxy groups of guaiacol as well as OH groups of guaiacol perturbed by silanols (Scheme 1, modes II to IV). As in the case of phenol, no stretching and bending OH groups of free guaiacol are detected, showing that these groups are perturbed by adsorption on silica. The low frequency region of the spectrum of adsorbed guaiacol is close to neat liquid guaiacol, indicating that it is weakly adsorbed on the surface by H-bonding. At the same time, the presence of shoulders at 1600 and 1508 cm^{-1} on the main bands at 1598 and 1504 cm^{-1}, respectively, may indicate the formation of new species. Some changes in the 1470−1444 cm^{-1} range cannot be clearly interpreted because of the presence of bands due to CH_3 and OH vibrations.

After evacuation at 373 K, characteristic $\nu(CC_{ring})$ vibrations (1600 and 1508 cm^{-1}) are still observed, but the δ(OH) contribution at 1366 cm^{-1} disappears. This shows that guaiacol, like phenol, forms methoxyphenate species at low temperature, probably through similar mechanism. These species are quite stable on silica and may be observed even after evacuation at 673 K (Figure 1, spectrum c_2).

Oxygenated Molecules on Alumina. ***Phenol Adsorption on Alumina.*** On alumina, phenol mainly forms phenate species as evidenced, Figure 2, by bands of aromatic ring vibrations (1597 and 1498/1492 cm^{-1}), ν(CO) bands (1295/1250 cm^{-1}), and the absence of specific δ(OH) vibrations (∼1470 and ∼1340 cm^{-1}) except at high coverage (Figure 2, spectrum b).[11,12,26] The

SCHEME 2: Different Structures of Phenate Species on Alumina

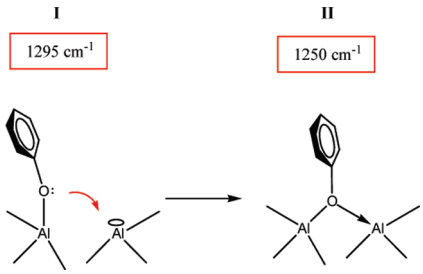

presence of a doublet at 1498/1492 cm^{-1} cannot be attributed to H-bonded phenol and phenate species as proposed for silica because of the absence of physisorbed phenol. However, the various components at 1498/1492 and 1295/1250 cm^{-1} lead us to propose the formation of two phenate species, mono- and bidentate, as illustrated in Scheme 2.

As previously reported,[30] methanol on zirconia forms mono- (type I) and bidentate (type II) methoxy species with characteristic ν(CO) vibrations at 1160 and 1060 cm^{-1}. However, for methanol on alumina, only one type of species is reported to be stable under high-temperature evacuation, bridged methoxy groups.[31] The structural differences between methoxy species formed on zirconia and alumina may be explained by the stronger Lewis acidity of the Al^{3+} as compared to the Zr^{4+} sites;[32] that can favor the transformation of type I into type II methoxy groups by the interaction of the basic oxygen atom of a monodentate methox with a neighboring Al^{3+}. The lower basicity of the phenate as compared to the methoxy oxygen should partially limit the transformation of type I into type II phenoxy species on alumina. Hence, both type I and type II phenoxy species are expected on alumina, whereas mainly type II methoxy species should be observed. That is in agreement with experimental data.

For the adsorption of small quantities of phenol, the δ(OH) vibration is not observed. The formation of H-bonded species only occurs at high phenol coverage (Figure 2, spectrum b), as indicated by the shoulder at ~1470 cm^{-1} characteristic of phenolic δ(OH). Thus, at RT and above, phenol mainly reacts with alumina to form phenate species. The perturbation of alumina OH groups should be related to the presence of chemisorbed species. Phenate formation likely occurs through a dissociative adsorption mechanism, requiring the presence of acid−base paired sites, that is (Al^{3+} and O^{2-}), as described in Scheme 3A. Similar mechanisms were previously proposed for alcohols adsorption on alumina.[33,34] Spectra taken after evacuation at 373 and 673 K (Figure 2, c_1 and c_2) show that phenate species are strongly adsorbed on alumina since they can be observed, even after evacuation at 723 K.

Anisole Adsorption on Alumina. When anisole interacts at RT with alumina, aromatic ring vibration bands shift (Figure 4). The presence of Lewis sites may be responsible for this effect, through donor−acceptor interaction between a surface Lewis site and the oxygen of anisole (Figure 4, spectrum b). The shoulders at ~1600 and ~1500 cm^{-1} may indicate the presence of weakly adsorbed anisole along with coordinated species.

After evacuation at elevated temperatures (Figure 4, spectrum c_2), the aromatic ring vibrations of anisole are very close to those of phenol. At the same time, bands related to vibrations of CH_3 and CH groups (3000−2800 cm^{-1}) are still detected. Apparently, transformation of donor−acceptor species formed at RT leads to the formation of phenate and methoxy species.

Anisole decomposition may proceed through the breakage of either Ph−OCH_3 or of PhO−CH_3 bonds. When anisole is adsorbed on ^{18}O-exchanged alumina (data not shown), no species corresponding to phenates-^{18}O are detected. However, unfortunately, the band of ^{18}O-methoxy groups on this oxide is

SCHEME 3: Interaction on Alumina: (A) Phenol, (B) Anisole, and (C) Guaiacol

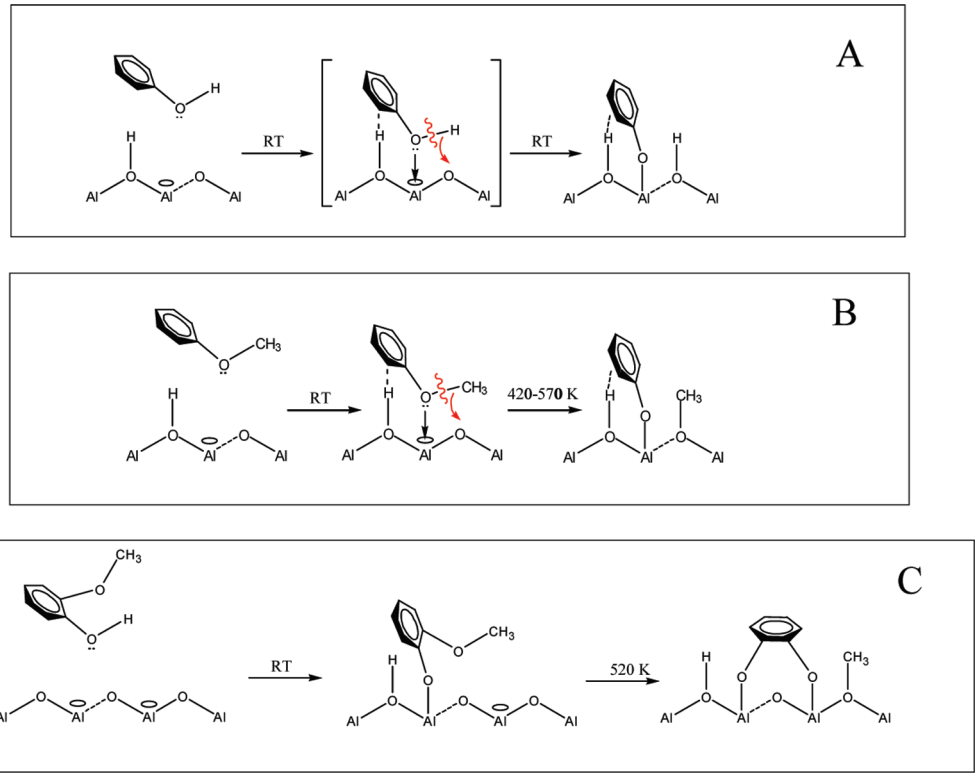

TABLE 3: Modes of Interaction of Phenol, Anisole, and Guaiacol with Oxides

	SiO_2	Al_2O_3	$SiO_2-Al_2O_3$
phenol	H-bonding and phenate formation	phenate formation from RT	H-bonding and phenate formation
anisole	H-bonding	coordination at RT and phenate formation from 473 K	phenate formation from $T > 573$ K
guaiacol	H-bonding and chemisorption as methoxyphenate	chemisorption as doubly anchored phenate at RT	ND

located at very low wavenumber, and its position is too close to the structural vibration bands of alumina to unambiguously conclude on the formation of methoxy-^{18}O species. Additional experiments with anisole adsorbed on zirconia, since zirconia presents structural vibration bands at lower frequencies than alumina and ^{18}O-exchanged zirconia (not shown) confirm the exclusive formation of phenate-^{16}O species [$\nu(C^{16}O)$ at 1283 cm^{-1}]. In this case, the presence of terminal methoxy-^{18}O species [$\nu(C^{18}O)$ band at 1114 cm^{-1}] is clear. Therefore, the formation of phenates on alumina occurs through the coordination of anisole on Lewis sites followed by cleavage of the $PhO-CH_3$ bond and migration of the CH_3 to surface oxygen, as described in Scheme 3B.

Guaiacol Adsorption on Alumina. The presence of all of the guaiacol bands upon adsorption indicates weakly bonded molecular guaiacol on the surface (Figure 5). The perturbation of the alumina and guaiacol OH groups also confirms an H-bonding type of interaction. However, new bands at 1330 and 1300 cm^{-1} may be attributed to the formation of another species along with H-bonded guaiacol. Evacuation even at RT (data not shown) leads to the total disappearance of the guaiacolic OH group (1366 cm^{-1}), while the other characteristic bands of guaiacol are still very intense. This is in agreement with the formation of new species having no OH groups, that is, methoxyphenates. Hence, one could expect that methoxyphenates give rise to several $\nu(CO)$ bands in the 1330−1200 cm^{-1} zone, which characterizes methoxy groups as well as type I and type II phenate species (as observed with phenol, although with different wavenumbers because of the methoxy group presence). After evacuation at 673 K, band characterizing $\delta(CH_3)$ vibrations (1470−1444 cm^{-1}) and that at 1225 cm^{-1} that should be assigned to $C-OCH_3$ ones are eliminated (Figure 5, spectrum c_2). Hence, although methoxyphenates formed on silica are not transformed further when temperature increases, changes occur on alumina. Thus, we propose that methoxy groups react with alumina Lewis sites at elevated temperatures. This is supported by the fact that anisole reacts with alumina at similar temperature (423−473 K) by forming phenate species. Although a complete interpretation of all spectral transformation is difficult, the formation of doubly anchored species between guaiacol and alumina is very likely (Scheme 3C).

Effect of Acidic Properties of the Oxide on the Adsorption of Oxygenated Molecules. As summarized in Table 3, the present work shows the influence of the nature of the oxide on the adsorption modes of the three oxygenated molecules. Indeed, silica possesses only very weak acidic OH groups, whereas alumina displays additional strong and medium Lewis acid sites.[35] The influence of Brønsted acidity on the interaction of these oxygenated molecules arises. The three oxygenated molecules were also adsorbed on an ASA presenting both strong and medium Lewis acidic sites, very weak acidic OH groups, and some strong acidic OH groups.[36]

Phenol Adsorption on Silica, Alumina, and ASA. Figure 6 compares the IR spectra of phenol adsorption on ASA to those obtained on pure silica and alumina. At low coverage (Figure 6A), the intensity of the band specific of molecular phenol species (1474 cm^{-1}) on ASA shows phenol interacting via H-bonding (that was the main adsorption mode at RT on silica) and being dissociatively adsorbed (main adsorption mode at RT on alumina). At higher coverage (Figure 6B), the spectrum on silica−alumina is closer to that of silica, likely due to its high silica content (88 wt % SiO_2). After evacuation at high temperature (Figure 6C), all of the spectra present only bands related to phenate species, its amount following the order: $Al_2O_3 \gg ASA > SiO_2$, that is, showing that anchored species are directly related to the Lewis acidity.

Adsorption of Anisole on Silica, Alumina, and ASA. Figure 7 compares anisole adsorption on the three supports. The first anisole molecules coordinate to the Lewis acid sites of ASA; because the aluminum content of the ASA is low, these sites are rapidly saturated and subsequent anisole molecules interact via H-bonding. After high evacuation temperature (Figure 7C), phenate species form on the alumina and silica−alumina. Furthermore, the amount of chemisorbed species on ASA is lower than on alumina. As for phenol, the formation of phenate species is related to the amount of Lewis sites of the oxide.

The presence of a small concentration of Brønsted acid sites, on ASA, does not induce a new mode of adsorption or further degradation of the oxygenated molecules. This demonstrates that the key point in the formation of carbonaceous fragments strongly held on the surface is the concentration of Lewis sites of the support.

It is, however, still unclear whether only Lewis acid sites or Lewis acid−base pairs are responsible for the strong adsorption of oxygenates on oxides. The proposed mode of interaction (Scheme 3) includes the formation of a donor−acceptor complex with a Lewis acid site followed by the transfer of a proton or methyl group to a Lewis basic site. To determine the rate-limiting step, additional alumina samples promoted by potassium (Al_2O_3-K) and fluorine (Al_2O_3-F) were studied.

Adsorption of Phenol on Al_2O_3-K and Al_2O_3-F. Pyridine adsorption measurements (not shown) provide evidence that fluorine addition does not change the Lewis acid sites concentration in comparison with the pure alumina but increases their strength. In contrast, potassium addition greatly decreases their concentration. CO_2 adsorption performed on these systems indicates a marked diminution of the Lewis basic site concentration of Al_2O_3-F[37] and a small increase of the basic site concentration of Al_2O_3-K.[37,38]

Phenol adsorbed at RT (data not shown) on Al_2O_3 and Al_2O_3-K leads only to phenate species. On Al_2O_3-F, the presence of phenolic OH groups shows that molecular phenol is H-bonded. So, a decrease of alumina basicity leads to the suppression of the dissociative adsorption at RT and confirms the importance of the second step of adsorption, that is, stabilization by proton transfer to the basic site.

Figure 3 shows the spectra of pure and doped (Al_2O_3-K and Al_2O_3-F) alumina samples after adsorption and evacuation of phenol at 573 K. At this temperature, all of the samples display only phenate species. The relative intensity of the ~1298 (type I monodentate) and 1245 cm^{-1} (type II bidentate) bands shows that for Al_2O_3-K, only type I species are formed, while for Al_2O_3-F, the concentration of type II species is more important than on pure alumina. According to Scheme 2, the suppression

TABLE 4: Concentrations (μmol g^{-1}) of the Adsorbed Species after Oxygenate Treatment Followed by Evacuation at 673 K

	SiO_2	Al_2O_3	$SiO_2-Al_2O_3$
phenol	91[a]	706	157[a]
anisole[a]	0	654	26[a]

[a] The molar absorption coefficient of phenate species on Al_2O_3 is used since under these conditions of adsorption only phenates are formed.

of type II on Al_2O_3-K may be due to the poisoning of strong Lewis acid sites, making impossible their formation. The greater ratio type II/type I phenate species on Al_2O_3-F vs Al_2O_3 is in good agreement with stronger Lewis acid sites on this sample.

The present study highlights that modifications of the acid−base properties of alumina (by doping with K or F) influence the structure of phenate species formed but do not prevent their formations. On the other hand, silica addition markedly decreases the phenate species amount. Hence, to minimize the presence of strongly held carbonaceaous species, silica-containing oxides are candidates worth considering to design HDO catalysts.

Comparison of the Amounts of Oxygenated Compounds Adsorbed. Using the value of molar absorption coefficient of the ring vibration band at 1600 cm^{-1} calculated in section 4.4 (ε_{1600} is 5.46 cm μmol^{-1}), the amounts of phenate species on silica, alumina, and silica−alumina are calculated (Table 4).

In a first step, the amount of Lewis acidic sites detected by pyridine adsorption[39] on alumina was compared to the amount of phenate formed. Because these amounts are consistent (close to 700 μmol g^{-1} in both cases), this validates the value of the molar absorption coefficient of phenate species.

The amount of phenate present on alumina for a temperature typical of the HDO reaction (673 K) reaches 706 μmol g^{-1} that corresponds to ~1.5 phenate per square nanometer. Considering the van der Waals radius of the phenyl group (0.74 nm), a simple calculation of the surface occupied by one phenate can be done. In this model, the maximum density of adsorbed phenate should be 2.3 molecules per nm^2. That means that at the temperature of the reaction, two-thirds of the alumina surface is covered by phenate species.

Among the oxides, the largest concentration of phenate species is formed on alumina for phenol and anisole (Table 4). Unfortunately, for guaiacol, no quantitative data could be obtained. However, the strength of species formed from guaiacol interaction is clearly stronger than for phenol and anisole adsorption.

In conclusion, catalyst supported on alumina is more susceptible to deactivation by oxygenated compounds. Adding silica to alumina could be a way to limit deactivation.

Conclusion

This contribution investigates the influence of acid−base properties of oxides on the adsorption modes of phenolic type molecules. Phenol, anisole, and guaiacol mainly interact via H-bonding with silica. By contrast, chemisorption is their main adsorption mode on alumina. Molecules containing a phenolic function (phenol and guaiacol) form phenate species already at RT. On the other hand, anisole requires temperature greater than 473 K to transform coordinated species into phenate species. Phenol and anisole are chemisorbed on alumina as phenates, whereas guaiacol strongly interacts by forming doubly anchored phenates. Modifications of the acid−base properties of alumina (by doping with K or F) change the nature of phenate species but do not prevent their formations. By contrast, silica addition to alumina markedly decreases the presence of phenate species.

For the first time, the molar absorption coefficient of phenate species is determined. Quantitative analysis shows that the phenate species covered at least two-thirds of the alumina surface at reaction temperature. Thus, alumina-based oxides are particularly reactive toward oxygenated compounds. The formation of these carbonaceous species, most probably "coke" precursors, is related to the presence of Lewis acid−base pairs on the alumina surface.

HDO catalysts are composed of an active phase (generally a mixed sulfide phase) deposited on an oxide (generally alumina). The present study shows that the strong interaction between the phenolic compounds and the alumina support could be a source of severe catalyst poisoning. Silica-containing alumina supports appear as a good alternative provided that a high dispersion of the active phase could be achieved. Further work, using the methodology developed in this contribution, is in progress to monitor the behavior of fresh and used catalysts based on mixed (CoMo) sulfides deposited on alumina and alternative supports.

Acknowledgment. This work has been performed within ECOHDOC, a joint project between CNRS, Universities of Caen, Lille and Poitiers, and Total, funded by the ANR (Programme National de Recherche sur les Bioénergies).

References and Notes

(1) Furimsky, E. *Appl. Catal., A* **2000**, *199*, 147.
(2) Elliott, D. C. *Energy Fuels* **2007**, *21*, 1792.
(3) Laurent, E.; Delmon, B. *Stud. Surf. Sci. Catal.* **1994**, *88*, 459.
(4) Laurent, E.; Delmon, B. *J. Catal.* **1994**, *146*, 281.
(5) Senol, O. I.; Viljava, T. R.; Krause, A. O. I. *Catal. Today* **2005**, *106*, 186.
(6) Odebunmi, E. O.; Ollis, D. F. *J. Catal.* **1983**, *80*, 56.
(7) Centeno, A.; Laurent, E.; Delmon, B. *J. Catal.* **1995**, *154*, 288.
(8) Laurent, E.; Centeno, A.; Delmon, B. *Stud. Surf. Sci. Catal.* **1994**, *88*, 573.
(9) Ballerini, D. *Les Biocarburants*; Technip ed: Paris, France, 2006.
(10) Balfour, W. J. *Spectrochim. Acta, Part A* **1983**, *39*, 795.
(11) Evans, J. C. *Spectrochim. Acta* **1960**, *16*, 1382.
(12) Roth, W.; Imhof, P.; Gerhards, M.; Schumm, S.; Kleinermanns, K. *Chem. Phys.* **2000**, *252*, 247.
(13) Hair, M. L.; Hertl, W. *J. Phys. Chem.* **1969**, *73*, 4269.
(14) Sempels, R. E.; Rouxhet, P. G. *Bull. Soc. Chim. Belges* **1975**, *84*, 361.
(15) Verma, V. N.; Nair, K. P. R.; Rai, D. K. *Isr. J. Chem.* **1970**, *8*, 777.
(16) Cusumano, J. A.; Low, M. J. D. *J. Catal.* **1971**, *23*, 214.
(17) Rochester, C. H.; Trebilco, D. A. *J. Chem. Soc. Faraday Trans. I* **1978**, *74*, 1125.
(18) Rochester, C. H.; Trebilco, D. A. *J. Chem. Soc. Faraday Trans. I* **1978**, *74*, 1137.
(19) Rupprecht, V. H.; Fuchs, G. *Pharm. Ind.* **1978**, *40*, 1174.
(20) Saracual, A. R. A.; Rochester, C. H. *J. Chem. Soc. Faraday Trans. I* **1982**, *78*, 2787.
(21) Scire, S.; Crisafulli, C.; Maggiore, R.; Minico, S.; Galvagno, S. *Appl. Surf. Sci.* **1996**, *93*, 309.
(22) Shabalin, I. I.; Kiva, E. A.; Churkin, Y. V.; Rusanova, L. A.; Mazitov, M. F. *Kinet. Catal.* **1974**, *15*, 1360.
(23) Tanabe, K.; Hölderich, W. F. *Appl. Catal., A* **1999**, *181*, 399.
(24) Taylor, D. R.; Ludlum, K. H. *J. Phys. Chem.* **1972**, *76*, 2882.
(25) Xu, B. Q.; Yamaguchi, T.; Tanabe, K. *Mater. Chem. Phys.* **1988**, *19*, 291.
(26) Taylor, D. R.; Ludlum, K. H. *J. Phys. Chem.* **1972**, *76*, 2882.
(27) Bazin, P.; Alenda, A.; Thibault-Starzyk, F. *Dalton Trans.* DOI: 10.1039/b00000000x.
(28) Travert, A.; Manoilova, O. V.; Tsyganenko, A. A.; Maugé, F.; Lavalley, J. C. *J. Phys. Chem. B* **2002**, *106*, 1350.
(29) Morterra, C.; Magnacca, G.; Bolis, V. *Catal. Today* **2001**, *70*, 43.
(30) Bensitel, M.; Moravek, V.; Lamotte, J.; Saur, O.; Lavalley, J. C. *Spectrochim. Acta, Part A* **1987**, *43A*, 1487.

(31) Busca, G.; Rossi, P. F.; Lorenzelli, V.; Benaissa, M.; Travert, J.; Lavalley, J. C. *J. Phys. Chem.* **1985**, *89*, 5433.
(32) Lahousse, C.; Aboulayt, A.; Maugé, F.; Bachelier, J.; Lavalley, J. C. *J. Mol. Catal.* **1993**, *84*, 283.
(33) Travert, J.; Lavalley, J. C.; Saur, O. *J. Chim. Phys. Phys.-Chim. Biol.* **1981**, *78*, 27.
(34) Benaissa, M.; Saur, O.; Lavalley, J. C. *Mater. Chem.* **1982**, *7*, 699.
(35) Lahousse, C.; Maugé, F.; Bachelier, J.; Lavalley, J.-C. *J. Chem. Soc., Faraday Trans.* **1995**, *91*, 2907.
(36) Crepeau, G.; Montouillout, V.; Vimont, A.; Mariey, L.; Cseri, T.; Maugé, F. *J. Phys. Chem. B* **2006**, *110*, 15172.
(37) Can, F.; Travert, A.; Ruaux, V.; Gilson, J. P.; Maugé, F.; Hu, R.; Wormsbecher, R. F. *J. Catal.* **2007**, *249*, 79.
(38) Mey, D.; Brunet, S.; Canaff, C.; Maugé, F.; Bouchy, C.; Diehl, F. *J. Catal.* **2004**, *227*, 436.
(39) Khabtou, S.; Chevreau, T.; Lavalley, J. C. *Microporous Mater.* **1994**, *3*, 133.

JP101949J